

Analysis of a flat plate collector for hot water domestic use – a sensitivity study

C Stanciu¹, D Stanciu¹, A Gheorghian¹ and I Şoriga¹

¹Engineering Thermodynamics Department, Faculty of Mechanical Engineering and Mechatronics, University POLITEHNICA of Bucharest, Bucharest, Romania

E-mail: camelia.stanciu@upb.ro

Abstract. The paper presents the study of a flat plate collector (FPC) used to heat water for domestic use in stationary operation. A comparison is provided between the cases of constant and time-dependent water circuit, in clear sky conditions. Numerical results emphasize the hot water temperature obtained with a given FPC area for a certain value of the mass flow rate. Imposing both the mass flow rate and hot water temperature, the minimum required area of the FPC can be determined. The computations are based on energy and mass balance equations. Steady state is obtained after three days of continuous operation.

1. Introduction

There is a spreading out of studies dedicated to flat plate collectors (FPC) in the recent time and so many products delivered to the market for producing domestic hot water using solar energy.

Duffie and Beckman [1] present thermodynamic modelling of different types of solar collectors and particular of flat plate collectors, and also cases studied in some papers dedicated to flat plate collectors.

Kalogirou [2] presented a useful review on solar thermal collectors, their applications and range data. Flat plate collectors are categorized as stationary collectors, having unity concentration ratio and temperature range use for standard collectors between 30-80°C, heating water, air or other gases [2]. Highly selective coatings may be used to reach higher temperatures. A mass flow rate of 0.015 kg/s/m² is given as FPC characteristic [2].

Raja Sekhar et.al. [3] presented a method and experimental setup to calculate the top loss coefficient of water FPC. Values between 2.5 and 7 W/K/m² are reported for different absorber plate temperatures and plate emissivity.

Luminosu and Fara [4] studied the optimisation of FPC from exergetic efficiency point of view and found for Romania the following optimum operation point at the average radiant power density of 550 W/m²: 3.5 m² FPC area, heating 0.0061 kg/s water from ambient temperature to 60°C. A maximum value of 78°C is reported between 12 AM and 2 PM. The FPC heat loss coefficient was considered constant and equal to 4.77 W/K/m². A cylinder shape storage tank of 200 kg water was considered.

A study was performed by Adnan et.al. [4] focusing on the effect of a fully mixed storage tank volume and working fluids mass flow rates on the efficiency of a 1.8 m² hybrid solar collector in Romania's climatic conditions. An optimum from daily efficiency point of view was found for a hot-water storage tank volume of 400 L and a water mass flow rate of 0.14 kg/s at 0 kg/s air mass flow rate.



3. Thermal model

The thermal model consists in applying mass balance and energy balance equations to the studied system and components.

The mathematical expression of the First Law of Thermodynamics (energy balance equation) for a control volume, neglecting variations of kinetic and potential energies, is

$$\frac{dU}{d\tau} = \sum_i \dot{m}_i h_i - \sum_o \dot{m}_o h_o + \dot{Q} - \dot{W} \quad (1)$$

The following hypotheses are considered:

- Solar radiation is determined by applying Hottel & Woertz model in clear sky conditions[1];
- Measured data for ambient temperature are used[9];
- Time dependent computations of the flat plate collector; time dependent global heat transfer coefficient and constant mass flow rate inside FPC; constant tilt all along the period, according to [10];
- Constant mass of water inside the storage tank and uniform temperature distribution;
- Constant global heat transfer coefficient for the storage tank;
- Time dependent fluid properties, computed in EES environment [11].

Equation (1) is applied for the flat plate collector considering convection, conduction through insulation and radiation heat losses, and for the storage tank in transient operation so that inside water temperature variation in time is determined.

3.1. Incoming solar energy

As input energy to the system, solar energy is used. Hottel & Woertz model is applied in clear sky conditions, as presented by [1] and previously applied by the authors for similar studies involving solar radiation density in Romania [10].

Total solar radiation is computed based on direct and diffuse components, considering atmospheric transmittance, as follows:

$$I_T = I_B + I_D \quad (2)$$

Direct component of the solar radiation is computed for the n th day of the year as:

$$I_B = \underbrace{\left(a_0 + a_1 e^{-\frac{k}{\cos \theta_z}} \right)}_{\tau_B} I_{SC} \left(1 + 0.033 \cos \frac{360n}{365} \right) \cos \theta \quad (3)$$

and diffuse one as:

$$I_D = (0.271 - 0.294\tau_B) I_{SC} \left(1 + 0.033 \cos(360n/365) \right) \cos \theta_z \quad (4)$$

where $I_{SC} = 1367 \text{ Wm}^{-2}$ represents the solar constant;

$\cos \theta$ is the angle of incidence of beam radiation on the FPC surface which is oriented towards South;

it is computed function on declination $\delta = 23.45 \sin \left(360 \frac{284 + n}{365} \right)$ [11], latitude φ , tilt angle of the FPC β and hour angle $\omega = 15^\circ \times (\text{time} - 12)$:

$$\cos \theta = \sin \delta \sin \varphi \cos \beta - \sin \delta \cos \varphi \sin \beta + \cos \delta \cos \varphi \cos \beta \cos \omega + \cos \delta \sin \varphi \sin \beta \cos \omega \quad (5)$$

In equation (4), $\cos \theta_z$ is computed for a horizontal surface ($\beta=0$).

The simulation can be done whatever the day of the year and the solar time. For the numerical simulation a 10 minutes step for time variation was considered.

3.2. Mass flow rate to the user

The above described solar radiation is used to heat water. Two cases are considered.

In the first case, a constant flow rate of 3l/h is considered to be delivered all day long. It is suited for a small-scale industrial application, for example.

In the second case, a time-dependent flow rate profile is taken into account. The hot water consumption profile was established by correlation with the electricity consumption profile, for an ordinary family of four, two adults and two children. No differences were considered between the hot water consumption in summer and winter. The tapping cycle was obtained based on the third domestic hot water demand profile presented in the European Union mandate for the elaboration and adoption of measurement standards for household appliances EU M324EN [13]. This profile, which requires 24 draws per day, amounting to a total volume of 200 L of water at 60°C, was modified to suit the particular case analyzed. The amount of hot water for each specific extraction and water temperature were determined according to the guide values specified by F. Späte and H. Ladener [13]. In both cases it was assumed that the tap water temperature is equal to 10°C, and the consumer water mass flow rate is 3.5 L/min. For a working day the total needed volume of hot water at 60°C was 184.4 L.

The variation presented in figure 2 was obtained.

3.3. Flat plate collector modelling

An ordinary flat plate collector is considered [10], [14]. The total incident solar radiation passes through a glass cover and reaches a black absorber plate in which liquid tubes are mounted in an insulation bed.

The absorbed solar radiation I_{Ab} is calculated considering the cover-absorber property $(\tau\alpha)=0.8$:

$$I_{Ab} = (\tau\alpha)I_T A_p \quad (6)$$

The plate area is $A_p = 1\text{m}^2$.

The useful thermal load of the FPC is computed considering convection and radiation losses through the top of the FPC cover:

$$\dot{Q}_u = A_p [I_{Ab} - U_L (T_p - T_a)] \quad (7)$$

where the overall heat loss coefficient is:

$$U_L = \left(\frac{1}{h_{cv,p-c} + h_{rad,p-c}} + \frac{1}{h_{cv,c-a} + h_{rad,c-a}} \right)^{-1} \quad (8)$$

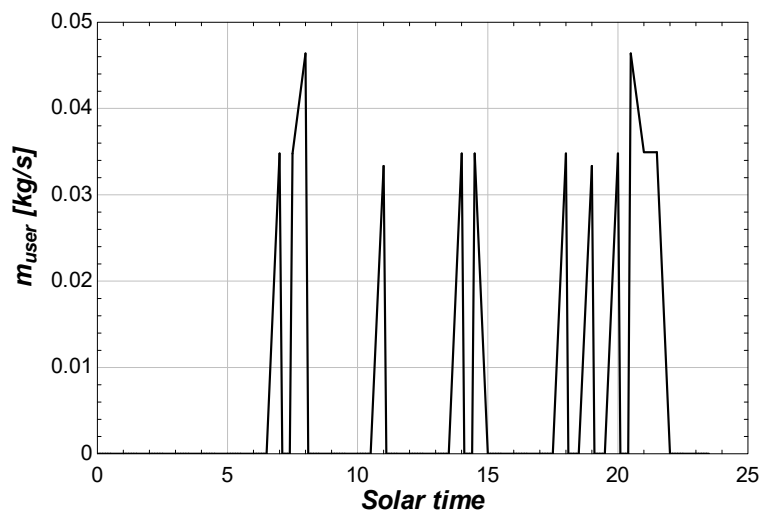


Figure 2. Time-dependent mass flow rate to user.

The losses between plate and cover (“*p-c*”) are computed as between two parallel plates[1], as follows: convection

$$h_{cv,p-c} = Nu \cdot k / L_{p-c} \quad (9)$$

and radiation:

$$h_{rad,p-c} = \sigma(T_p + T_c)(T_p^2 + T_c^2) \left(\frac{1}{\varepsilon_p} + \frac{1}{\varepsilon_c} - 1 \right)^{-1} \quad (10)$$

The plate emittance ε_p is 0.05 and the cover emittance ε_c is 0.89. The plate-cover distance L_{p-c} is 0.04m.

Nusselt number Nu is computed using [15]:

$$Nu = 1 + 1.44 \left[1 - \frac{1708(\sin 1.8\beta)^{1.6}}{Ra \cos \beta} \right] \left[1 - \frac{1708}{Ra \cos \beta} \right]^+ + \left[\left(\frac{Ra \cos \beta}{5830} \right)^{1/3} - 1 \right]^+ \quad (11)$$

Rayleigh number is computed between T_p and T_c .

The convection losses between cover and ambient (“*c-a*”) are due to wind forced convection [15]:

$$h_{cv,c-a} = 5.7 + 3.8w \quad (12)$$

and radiation between cover and ambient temperatures:

$$h_{rad,c-a} = \varepsilon_c \sigma(T_c + T_a)(T_c^2 + T_a^2) \quad (13)$$

In equations (7)-(13), mean plate temperature T_p , cover temperature T_a and overall heat loss coefficient are unknown. Thus the system of equations is completed by adding a new relation: heat losses passing from plate to cover $q_{cv,p-c} + q_{rad,p-c}$ are further transmitted through cover to ambient, and thus equal to $q_{cv,c-a} + q_{rad,c-a}$. Solving this system of equations, all unknowns are determined.

The useful thermal load is then transmitted to the working fluid inside the FPC tubes; its outlet temperature is determined as:

$$T_{f,o} = T_{f,in} + \frac{\dot{Q}_u}{(\dot{m}_{FPC} C_{p,FPC})} \quad (14)$$

A constant mass flow rate in the FPC is considered $\dot{m}_{FPC} = 0.013$ kg/s. The specific heat of the working fluid (water) is computed in EES environment at mean fluid temperature. The inlet fluid temperature $T_{f,in}$ is computed as explained in section 2, from the energy balance equation applied for the mixing process between the storage tank fluid $\dot{m}_{FPC} - \dot{m}_{user}$ and fresh water at ambient temperature \dot{m}_{user} .

3.4. Storage tank modelling

A storage tank of 100L water is considered, in which the temperature level T_{st} is uniformly distributed and time-dependent. Convection and conduction losses to the exterior are considered too as $(UA)_{st} = 11$ W/K. The storage tank temperature is computed by applying the First Law of Thermodynamics in unsteady state, for the case $\dot{m}_{FPC} > \dot{m}_{user}$:

$$(mc_p)_{st} \frac{dT_{st}}{d\tau} = \dot{m}_{FPC} c_{p,FPC} T_{f,o} - \dot{m}_{user} c_{p,st} T_{st} - (\dot{m}_{FPC} - \dot{m}_{user}) c_{p,st} T_{st} - (UA)_{st} (T_{st} - T_a) \quad (15)$$

or for the case $\dot{m}_{FPC} < \dot{m}_{user}$:

$$\left(\dot{m}c_p\right)_{st} \frac{dT_{st}}{d\tau} = \dot{m}_{FPC}c_{p,FPC}T_{f,o} - \dot{m}_{user}c_{p,st}T_{st} - (\dot{m}_{FPC} - \dot{m}_{user})c_{p,st}T_{st} - (UA)_{st}(T_{st} - T_a) \quad (16)$$

By integrating this equation over each time step interval, temperature T_{st} is determined at each moment.

4. Results and discussions

The first case numerically simulated was for a constant mass flow rate to the user, corresponding to 3l/h in volume flow rate. Results are plotted in figures 3 and 4.

In figure 3 one may notice the time variation for plate and cover temperatures (near ambient one), outlet fluid temperature from FPC T_{fo} and storage tank temperature T_{st} . A smooth variation is emphasized and a maximum temperature of about 55°C is reached in the storage tank at July 15th (day number 196 in a whole year) around 4PM.

When the simulation was done for several consecutive days (in July and in March), steady-state operation was met after three days, as plotted in figures 4. By steady-state operation one should understand that the initial and final storage tank temperatures along a day are the same.

For the second case, namely time-dependent mass flow rate to the user, figures 5-7 were obtained.

In figure 5 one may notice the daily temperature variations of the plate, cover, outlet fluid from the FPC and storage tank fluid. Important differences are emphasized with respect to the previous studied case of constant mass flow rate to user. First of all, the profiles of the fluid curves are no longer smooth. Their steep variations correspond to the sharp variations of mass flow rate sketched in Figure 2. Secondly, the maximum storage tank temperature is of about 50°C at July 15th, around 5PM.

When plotting the inlet and outlet fluid temperatures in the FPC, in figure 6, there are several moments over a day when the inlet fluid temperature $T_{f,in}$ reaches the ambient temperature T_a . These periods correspond to the cases when $\dot{m}_{FPC} < \dot{m}_{user}$ and fresh water at ambient temperature is taken into the flat plate collector and into the storage tank. Thus, the outlet fluid temperature decreases and the storage tank temperature, too.

For several consecutive days' simulation, the same period of three days was emphasized for reaching steady-state, but the maximum temperature in the storage tank slightly decreased, as plotted in figure 7.

One may conclude that considering a time-dependent mass flow rate to user has important influences on the behaviour of a flat plate collector and simulations should be done consequently for a correct sizing of the system.

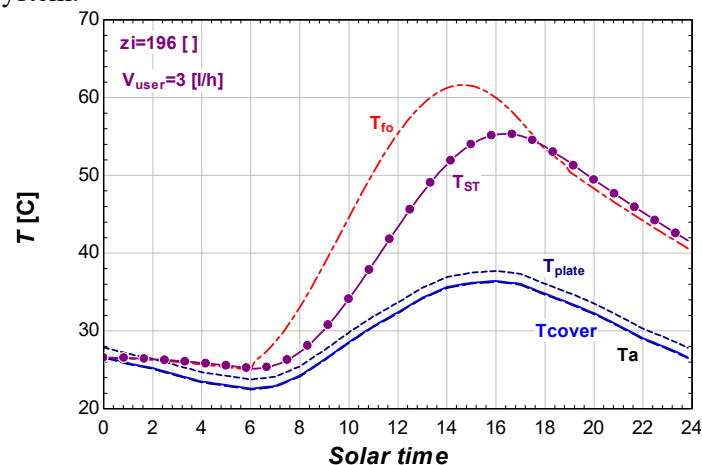


Figure 3. FPC cover and plate temperatures, fluid temperature at collector outlet and inside the storage tank at July 15th (constant flow rate to user).

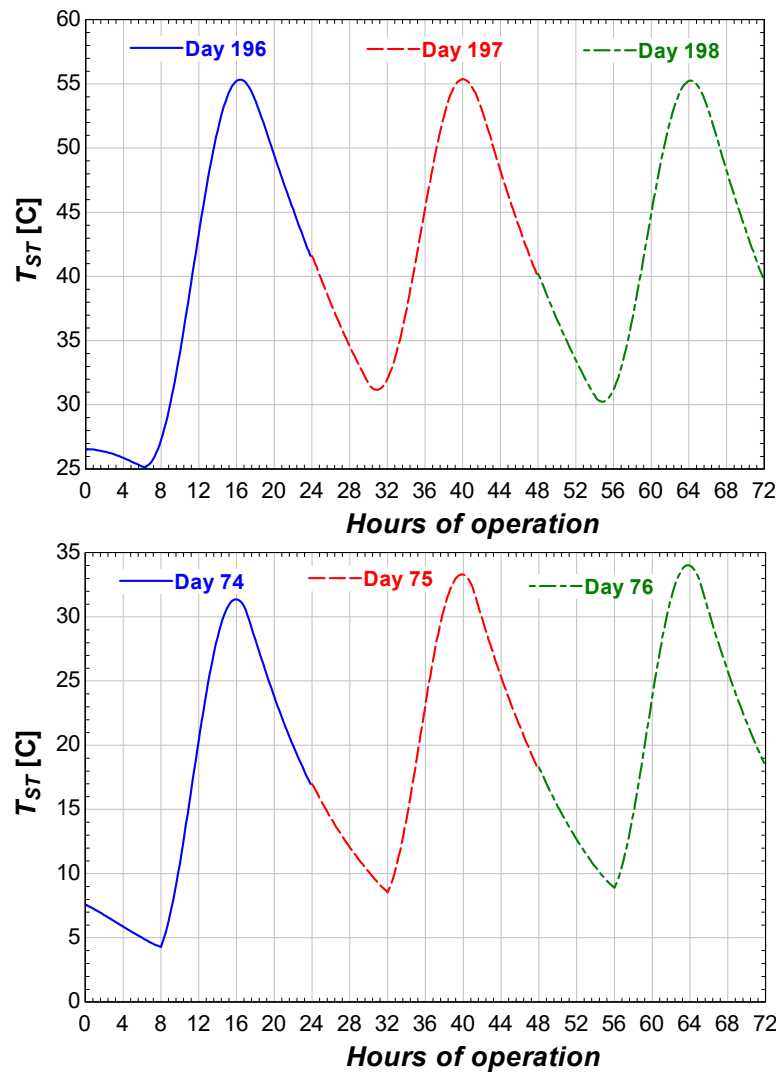


Figure 4. Fluid temperature inside the storage tank along 3 days (constant flow rate to user).

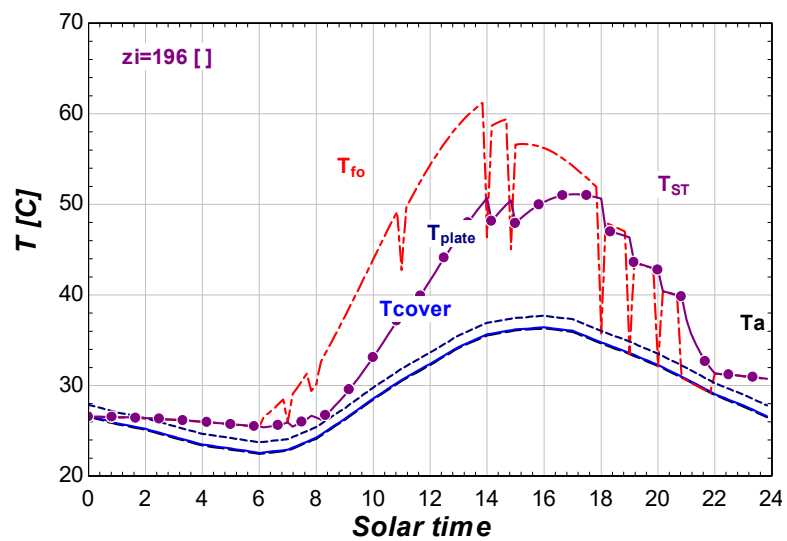


Figure 5. FPC cover and plate temperatures, fluid temperature at collector outlet and inside the storage tank at July 15th (time-dependent flow rate to user).

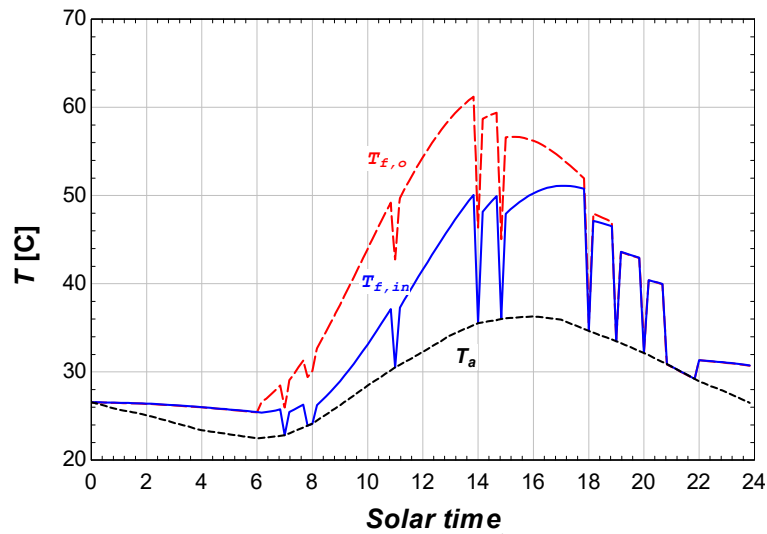


Figure 6. Inlet and outlet FPC fluid temperatures, at July 15th for considered time-dependent flow rate to user.

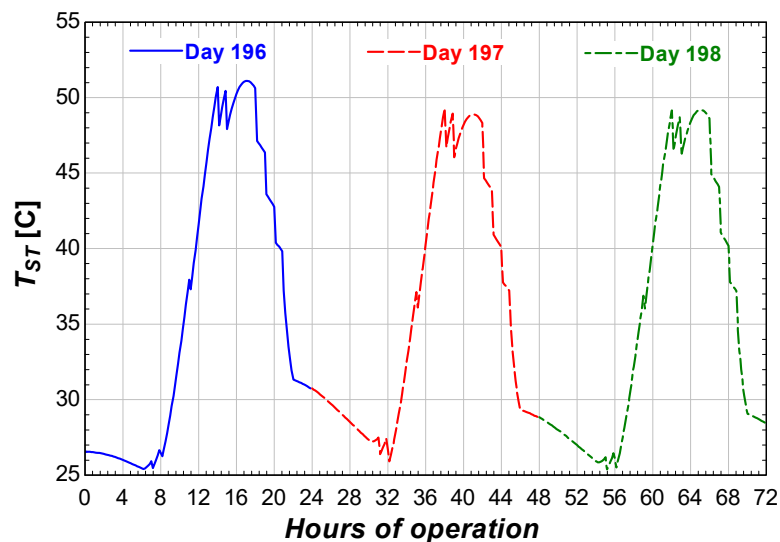


Figure 7. Fluid temperature inside the storage tank along 3 days (time-dependent flow rate to user).

5. References

- [1] Duffie JA and Beckman WA 2006 *Solar Engineering of Thermal Processes*, 3rd ed. (Hoboken:John Wiley & Sons)
- [2] Kalogirou SA 2004 Solar thermal collectors and applications *Progress in Energy and Combustion Science* **30** pp 231–295
- [3] Raja Sekhar Y, Sharma KV and Basaveswara Rao M 2009 Evaluation of heat loss coefficients in solar flat plate collectors *Journal of Engineering and Applied Sciences* **4(5)** pp 15-19
- [4] Luminosu I and Fara L 2005 Determination of the optimal operation mode of a flat solar collector by exergetic analysis and numerical simulation *Energy* **30** pp 731–747
- [5] Adnan Q, Badescu V and Soriga I 2015 Hybrid solar collector for water and air heating: effects of storage tank volume and air channel shape on efficiency *U.P.B. Sci. Bull., Series D77* (3) pp 29-40
- [6] Hamed M, Fellah A and Ben Brahim A 2014 Parametric sensitivity studies on the performance of a flat plate solar collector in transient behavior *Energy Conversion and Management* **78**

- pp 938–947
- [7] Dhariwal SR and Mirdha US 2005 Analytical expressions for the response of flat-plate collector to various transient conditions *Energy Conversion and Management* **46** pp 1809–1836
 - [8] Hottel HC and Woertz BB 1942 Performance of flat plate solar heat collectors *Trans. ASME* **64** pp 91
 - [9] Paulescu M, Dughir C, Tulcan-Paulescu E, Lascu M, Gravila P and Jurca T 2010 Solar Radiation Modeling and Measurements in Timisoara, Romania: Data and Model Quality *Environmental Engineering and Management Journal* **9(8)** pp 1089-1095
 - [10] Stanciu C and Stanciu D 2014 Optimum tilt angle for flat plate collectors all over the World – A declination dependence formula and comparisons of three solar radiation models *Energy Conversion and Management* **81** pp 133–143
 - [11] EES, Engineering Equation Solver, academic licence, V10.055-3D
 - [12] Cooper PI 1969 The absorption of solar radiation in solar stills *Solar Energy* **12(3)** pp 333-346
 - [13] European Commission, Mandate to CEN and CENELEC for the Elaboration and Adoption of Measurement Standards for Household Appliances: Water Heaters, Hot Water Storage Appliances and Water Heating Systems 2002 Brussels
 - [14] Späte F and Ladener H 2011 *Tehnica utilizării energiei solare. Manual de executie* (Bucharest: M.A.S.T.)
 - [15] Hollands KGT, Unny TE, Raithby GD and Konicek L 1976 Free convective heat transfer across inclined air layers *ASME J. Heat Transfer* **98** pp 189-193
 - [16] McAdams WH 1954, *Heat Transmission*, 3rd ed. (New York: McGraw Hill)

Acknowledgments

This work was supported by a grant of the Romanian National Authority for Scientific Research and Innovation, CNCS – UEFISCDI, project number PN-II-RU-TE-2014-4-0846.